Fault Tolerant Control Scheme Design for Formation Flight Control System of Multiple Unmanned Aerial Vehicles

Qian Moshu[1,2], *Xiong Ke*[2*]

1. College of Electrical Engineering and Control Science, Nanjing Tech University, Nanjing 211816, P. R. China;
2. State Key Laboratory of Mechanics and Control of Mechanical Structures, Nanjing University of Aeronautics and Astronautics, Nanjing 210016, P. R. China

(Received 18 January 2017; revised 20 February 2017; accepted 5 March 2018)

Abstract: The command tracking problem of formation flight control system (FFCS) for multiple unmanned aerial vehicles (UAVs) with sensor faults is discussed. And the objective of the addressed control problem is to design a robust fault tolerant tracking controller such that, for the disturbances and sensor faults, the closed-loop system is asymptotically stable with a given disturbance attenuation level. A robust fault tolerant tracking control scheme, combining an observer with H_∞ performance, is proposed. Furthermore, it is proved that the designed controller can guarantee asymptotic stability of FFCS despite sensor faults. Finally, a simulation of two UAV formations is employed to demonstrate the effectiveness of the proposed approach.

Key words: formation control; fault tolerant control (FTC); unmanned aerial vehicle (UAV); robust control

CLC number: TP273 **Document code**: A **Article ID**: 1005-1120(2018)04-0693-09

0 Introduction

An unmanned aerial vehicle (UAV) is an aircraft without a human pilot aboard. The flying of UAV, which depends on the flight control system (FCS) including actuator, sensor and so on, is controlled either autonomously by on board computers or by the remote control of a pilot[1-5]. The UAV not only has many potential military and civil applications but also has great scientific significance in academic research. One of the interesting topics is the cooperative control of UAV in formation flight, in which a group of UAVs fly in a desired graph formation[6-10]. There are reasons to believe that the efficiency of group performance is higher than that of single UAV. There have been significant researches in the area of cooperative control of multiple vehicles system in recent years. For examples, the authors mainly focused on the motion consensus and formation control of UAV swarm in Ref. [11], and a novel formation control algorithm suitable for both leaders and followers was designed, in which leaders can be influenced by feedback from their teammates. A normal PID control law was studied for the closed formation of UAVs in Ref. [12], and the bound condition of a safe distance was given. In Ref. [13], the authors respectively proposed centralized and decentralized event-triggered control laws, which achieved the the circle formation. The fault of single UAV or agent will influence the entire formation and even safe, so it is necessary to study the fault tolerant control (FTC) problem of the formation[14]. Several approaches have been exploited to solve the problem about accomplishing a certain formation for faulty UAVs. A mathematical model using dual quaternion is employed to describe the spacecraft formation. The effectiveness of the proposed control method is further demonstrated in the presence of actuator fault, disturbance and parameter uncertainty as well. Moreover, the finite-time stability of the

* Corresponding author, E-mail address: kxiong@nuaa.edu.cn.

How to cite this article: Qian Moshu, Xiong Ke. Fault tolerant control scheme design for formation flight control system of multiple unmanned aerial vehicles[J]. Trans. Nanjing Univ. Aero. Astro., 2018, 35(4):693-701.
http://dx.doi.org/10.16356/j.1005-1120.2018.04.693

closed-loop system is guaranteed by the adaptive feedback FTC law[15]. The authors investigate the time varying fault tolerant control formation problem for high-order multi-agent systems with actuator failure in Ref. [16]. Using the adaptive online updating strategies, the bounds of actuator failures can be unknown. Then an algorithm is proposed to determine the control parameters of the FTC, where an approach to expand the feasible formation set and the formation feasible conditions is given. A fault tolerant formation control scheme of UAV based on Kalman filter is presented, which can deal with both GPS sensor failure and wireless communication packet losses in Ref. [17]. A centralized null space based approach is introduced to compose a complex mission for swarms. Bernulli model and Extended Gilbert model are employed to value the impact of the main packet loss in wireless networks[18]. The works mentioned above perform effectively in the design of formation controller, but the sensor faults in multi-UAV formation are not studied seriously. Once the attitude, velocity or position sensor of a UAV fails, the formation flight control system (FFCS) will be influenced, which motivates us to study further[19-21].

Motivated by the above discussion, the robust fault tolerant tracking control design is discussed in this paper for FFCS of multi-UAV in which sensor faults happen to a single UAV. The dynamics model of UAV formation including sensor faults and disturbances is established. Then an observer-based feedback control approach is employed. Finally, a simulation example is given to illustrate the validity of the proposed approach.

1 Problem Statement

In this study, the typical leader and wingman formation patterns are adopted, and a typical triangle formation of UAV is shown in Fig. 1[22].

The aerodynamic coupling effects are ignored for the simplicity, and then a linear state space model for the FFCS of UAV is obtained [12]

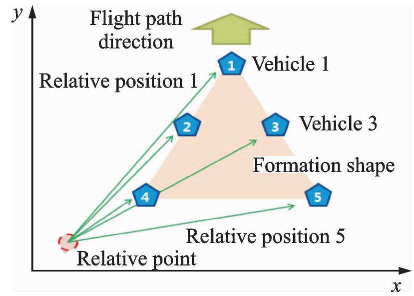

Fig. 1 Triangle formation of UAV

$$\begin{cases} \dot{\bar{\boldsymbol{x}}} = \boldsymbol{A}\bar{\boldsymbol{x}} + \boldsymbol{B}\boldsymbol{u} + \boldsymbol{\Theta}\boldsymbol{w}_1 \\ \bar{\boldsymbol{y}} = \boldsymbol{C}\bar{\boldsymbol{x}} \end{cases} \tag{1}$$

where

$$\bar{\boldsymbol{x}} = [x \quad V_W \quad y \quad \psi_W \quad z \quad \zeta]^{\mathrm{T}}$$

$$\boldsymbol{u} = \begin{bmatrix} V_{W_C} \\ \psi_{W_C} \\ h_{W_C} \end{bmatrix}, \boldsymbol{w}_1 = \begin{bmatrix} V_L \\ \psi_L \\ h_{L_C} \end{bmatrix}$$

$$\boldsymbol{A} = \begin{bmatrix} 0 & -1 & 0 & -y_0/\tau_{\psi_W} & 0 & 0 \\ 0 & -1/\tau_{V_W} & 0 & 0 & 0 & 0 \\ 0 & 0 & 0 & \left(\frac{x_0}{\tau_{\psi_W}} - V_{L_0}\right) & 0 & 0 \\ 0 & 0 & 0 & -1/\tau_{\psi_W} & 0 & 0 \\ 0 & 0 & 0 & 0 & 0 & 1 \\ 0 & 0 & 0 & 0 & -\frac{1}{\tau_{h_a}\tau_{h_b}} & -\left(\frac{1}{\tau_{h_a}} + \frac{1}{\tau_{h_b}}\right) \end{bmatrix}$$

$$\boldsymbol{B} = \begin{bmatrix} 0 & \frac{y_0}{\tau_{V_W}} & 0 \\ \frac{1}{\tau_{V_W}} & 0 & 0 \\ 0 & \frac{x_0}{\tau_{\psi_W}} & 0 \\ 0 & \frac{1}{\tau_{\psi_W}} & 0 \\ 0 & 0 & 0 \\ 0 & 0 & \frac{1}{\tau_{h_a}\tau_{h_b}} \end{bmatrix}, \boldsymbol{\Theta} = \begin{bmatrix} 1 & 0 & 0 \\ 0 & 0 & 0 \\ 0 & V_{L_0} & 0 \\ 0 & 0 & 0 \\ 0 & 0 & 0 \\ 0 & 0 & -\frac{1}{\tau_{h_a}\tau_{h_b}} \end{bmatrix}$$

where $\bar{\boldsymbol{x}}$, $\boldsymbol{u}$, $\bar{\boldsymbol{y}}$ and $\boldsymbol{w}_1$ are respectively state vector, control input, output vector and process disturbance vector. x, y and z are the separation distances between leader and follower with respect to the wing UAV. V_L, V_W are the leader and the follower velocities. ψ_L, ψ_W are the leader and the follower heading angles. $\boldsymbol{C} \in \mathbf{R}^{m\times 6}$ is a diagonal constant matrix, and m is a given positive constant. More parameters refer to Ref. [12].

In order to meet the requirements of actual conditions, the following important aspects should be taken into consideration simultaneously.

(1) Sensor fault. When the attitude, velocity or position sensor of a UAV occurs gain fault, the fault of FFCS will occur, and the measure values of x, y, z, ψ_W, V_W and ζ will fully or partially be inflected. Under this condition, the output can be generally characterized as[23]

$$\bar{\boldsymbol{y}}_F = \boldsymbol{F}\bar{\boldsymbol{y}} \tag{2}$$

where $\bar{\boldsymbol{y}}_F \in \mathbf{R}^q$ is the actual measure output of system in sensor faulty case, $\boldsymbol{F} \in \mathbf{R}^{q\times m}$ denotes the sensor gain fault parameter and satisfies the following inequality constraints: $0 \leqslant \underline{\boldsymbol{F}} = \mathrm{diag}\{\underline{f}_1, \underline{f}_2\} \leqslant \boldsymbol{F} = \mathrm{diag}\{f_1, f_2\} \leqslant \bar{\boldsymbol{F}} = \mathrm{diag}\{\bar{f}_1, \bar{f}_2\}$, $f_i (i=1,2)$ are the output proportion coefficients of system in sensor faulty case.

Here matrices $\boldsymbol{F}_0$ and $\tilde{\boldsymbol{F}}$ are given by

$$\boldsymbol{F}_0 = \mathrm{diag}\{f_{01}, f_{02}\} = \frac{\underline{\boldsymbol{F}} + \bar{\boldsymbol{F}}}{2} = \mathrm{diag}\left\{\frac{\underline{f}_1 + \bar{f}_1}{2}, \frac{\underline{f}_2 + \bar{f}_2}{2}\right\} \tag{3}$$

$$\tilde{\boldsymbol{F}} = \mathrm{diag}\{\tilde{f}_1, \tilde{f}_2\} = \frac{\bar{\boldsymbol{F}} - \underline{\boldsymbol{F}}}{2} = \mathrm{diag}\left\{\frac{\bar{f}_1 - \underline{f}_1}{2}, \frac{\bar{f}_2 - \underline{f}_2}{2}\right\} \tag{4}$$

The sensor fault model parameter $\boldsymbol{F}$ can be turned into

$$\boldsymbol{F} = \boldsymbol{F}_0 + \boldsymbol{F}_\delta = \boldsymbol{F}_0 + \mathrm{diag}\{\delta_1, \delta_2\} \tag{5}$$

where $\delta_i \leqslant \tilde{f}_i (i=1,2)$.

(2) Input constraint. In view of the limited power of actuator, the actual control input force should be confined into a certain range, which means that

$$\|\boldsymbol{u}(t)\|_2 \leqslant u_{\max} \tag{6}$$

where $u_{\max}$ denotes the maximum control input.

(3) Disturbance. In order to obtain an actual dynamic performance of FFCS, the disturbance vector $\boldsymbol{w}$, which includes process disturbance $\boldsymbol{w}_1$ and outside disturbance $\boldsymbol{w}_2$, is assumed to belong to a bounded set $\mathfrak{I}$ defined as $\mathfrak{I} \triangleq \{\boldsymbol{w} \in \triangleq^r : |\boldsymbol{w}| \leqslant \bar{\boldsymbol{w}}\}$ for some constant non-negative values $\bar{\boldsymbol{w}}$, that is, $\boldsymbol{w}(t) \in \mathfrak{I}$ for all time instants $t \geqslant 0$.

According to the above mentioned sensor faults and disturbances, the FFCS model (Eq. (1)) of UAV can be described by

$$\begin{cases} \dot{\bar{\boldsymbol{x}}} = \boldsymbol{A}\bar{\boldsymbol{x}} + \boldsymbol{B}\boldsymbol{u} + \boldsymbol{\Theta}\boldsymbol{w} \\ \bar{\boldsymbol{y}}_F = \boldsymbol{F}\bar{\boldsymbol{y}} = \boldsymbol{F}\boldsymbol{C}\bar{\boldsymbol{x}} \end{cases} \tag{7}$$

where $\boldsymbol{w}$ is a bounded disturbance.

To design the tracking controller, a reference model is introduced for FFCS

$$\dot{\bar{\boldsymbol{x}}}_r = \boldsymbol{A}_r\bar{\boldsymbol{x}}_r + \boldsymbol{r} \tag{8}$$

where $\bar{\boldsymbol{x}}_r \in \mathbf{R}^6$ is the reference state, $\boldsymbol{A}_r$ is a specified Hurwitz matrix and $\boldsymbol{r} \in \mathbf{R}^6$ is a bounded reference input.

Since UAV is a low cost aircraft and state variables are not all measured exactly, a close-loop system tracking controller based on an observer is designed as

$$\dot{\hat{\bar{\boldsymbol{x}}}} = \boldsymbol{A}\hat{\bar{\boldsymbol{x}}} + \boldsymbol{B}\boldsymbol{u} + \boldsymbol{L}(\bar{\boldsymbol{y}}_F - \hat{\bar{\boldsymbol{y}}}) \tag{9}$$

$$\hat{\bar{\boldsymbol{y}}} = \boldsymbol{C}\hat{\bar{\boldsymbol{x}}} \tag{10}$$

$$\boldsymbol{u} = -\boldsymbol{K}(\bar{\boldsymbol{x}}_r - \hat{\bar{\boldsymbol{x}}}) \tag{11}$$

where $\hat{\bar{\boldsymbol{x}}}$ is the estimated value of $\bar{\boldsymbol{x}}$, $\boldsymbol{L}$ the gain matrix of observer to be designed, and $\boldsymbol{K}$ an unknown control gain matrix with appropriate dimension.

The attenuation of external disturbances is guaranteed considering the H_∞ performance related to the tracking error $\bar{\boldsymbol{x}}_r - \bar{\boldsymbol{x}}$ as[24]

$$\int_0^{t_f} (\bar{\boldsymbol{x}}_r - \bar{\boldsymbol{x}})^{\mathrm{T}}\boldsymbol{Q}(\bar{\boldsymbol{x}}_r - \bar{\boldsymbol{x}})\mathrm{d}t \leqslant \eta^2\int_0^{t_f} (\boldsymbol{r}^{\mathrm{T}}\boldsymbol{r} + \boldsymbol{w}^{\mathrm{T}}\boldsymbol{w})\mathrm{d}t \tag{12}$$

where $\boldsymbol{Q}$ is a given positive definite weighting matrix, t_f denotes the final time, and η is a specified attenuation level. By defining the state estimated error $\boldsymbol{e}_0 = \bar{\boldsymbol{x}} - \hat{\bar{\boldsymbol{x}}}$, the tracking error $\boldsymbol{e}_p = \bar{\boldsymbol{x}} - \bar{\boldsymbol{x}}_r$, the state vector of the global closed-loop system $\tilde{\boldsymbol{x}} = [\boldsymbol{e}_0, \boldsymbol{e}_p, \bar{\boldsymbol{x}}_r]^{\mathrm{T}}$, then combining the control law (Eq. (11)), the system (Eq. (7)), and the observers (Eqs. (9), (10)), the following closed-loop system model can be obtained

$$\dot{\tilde{\boldsymbol{x}}} = \tilde{\boldsymbol{A}}\tilde{\boldsymbol{x}} + \tilde{\boldsymbol{B}}\tilde{\boldsymbol{\varphi}} \tag{13}$$

where

$$\tilde{\boldsymbol{A}}=\begin{bmatrix}\boldsymbol{A}-\boldsymbol{LC} & \boldsymbol{L}(\boldsymbol{I}-\boldsymbol{F})\boldsymbol{C} & \boldsymbol{L}(\boldsymbol{I}-\boldsymbol{F})\boldsymbol{C}\\ -\boldsymbol{BK} & \boldsymbol{A}+\boldsymbol{BK} & \boldsymbol{A}-\boldsymbol{A}_r\\ 0 & 0 & \boldsymbol{A}_r\end{bmatrix}$$

$$\tilde{\boldsymbol{S}}=\begin{bmatrix}\boldsymbol{\Theta} & 0\\ \boldsymbol{\Theta} & -\boldsymbol{I}\\ 0 & \boldsymbol{I}\end{bmatrix},\ \tilde{\boldsymbol{\varphi}}=\begin{bmatrix}\boldsymbol{w}\\ \boldsymbol{r}\end{bmatrix}$$

Note that with the state vector $\tilde{\boldsymbol{x}}$, in-Eq. (12) can be written with $\tilde{\boldsymbol{Q}}=\mathrm{diag}\{0,\boldsymbol{Q},0\}$

$$\int_0^t \tilde{\boldsymbol{x}}^{\mathrm{T}}\tilde{\boldsymbol{Q}}\tilde{\boldsymbol{x}}\,\mathrm{d}t \leqslant \eta^2\int_0^t \tilde{\boldsymbol{\varphi}}^{\mathrm{T}}\tilde{\boldsymbol{\varphi}}\mathrm{d}t \tag{14}$$

where $\tilde{\boldsymbol{\varphi}}^{\mathrm{T}}\tilde{\boldsymbol{\varphi}}=\boldsymbol{r}^{\mathrm{T}}\boldsymbol{r}+\boldsymbol{w}^{\mathrm{T}}\boldsymbol{w}$.

The objective is now to compute the gain matrices $\boldsymbol{K}$, $\boldsymbol{L}$ to ensure the asymptotic stability of Eq. (13) thus guaranteeing Eq. (14). A straightforward result is summarized in the following theorem.

Theorem 1 If there exists a matrix $\tilde{\boldsymbol{P}}=\tilde{\boldsymbol{P}}^{\mathrm{T}}>0$ and a positive constant η such that the following linear matrix inequality (LMI) is satisfied

$$\begin{bmatrix}\tilde{\boldsymbol{A}}^{\mathrm{T}}\tilde{\boldsymbol{P}}+\tilde{\boldsymbol{P}}\tilde{\boldsymbol{A}}+\boldsymbol{I} & \tilde{\boldsymbol{P}}\tilde{\boldsymbol{S}}\\ \tilde{\boldsymbol{S}}^{\mathrm{T}}\tilde{\boldsymbol{P}} & -\eta^2\boldsymbol{I}\end{bmatrix}<0 \tag{15}$$

then the asymptotic stability of the closed-loop formation control system Eq. (13) is ensured and the H_∞ tracking control performance Eq. (14) is guaranteed with an attenuation level η.

Proof Consider the following candidate Lyapunov function

$$V=\tilde{\boldsymbol{x}}^{\mathrm{T}}\tilde{\boldsymbol{P}}\tilde{\boldsymbol{x}}\qquad \tilde{\boldsymbol{P}}=\tilde{\boldsymbol{P}}^{\mathrm{T}}>0 \tag{16}$$

The stability of the closed-loop model (Eq. (13)) is satisfied under the H_∞ performance (Eq. (14)) with the attenuation level η if

$$\dot{V}+\tilde{\boldsymbol{x}}^{\mathrm{T}}\tilde{\boldsymbol{Q}}\tilde{\boldsymbol{x}}-\eta^2\tilde{\boldsymbol{\varphi}}^{\mathrm{T}}\tilde{\boldsymbol{\varphi}}\leqslant 0 \tag{17}$$

Eq. (17) leads to

$$\tilde{\boldsymbol{x}}^{\mathrm{T}}[\tilde{\boldsymbol{A}}^{\mathrm{T}}\tilde{\boldsymbol{P}}+\tilde{\boldsymbol{P}}\tilde{\boldsymbol{A}}+\tilde{\boldsymbol{Q}}]\tilde{\boldsymbol{x}}+\tilde{\boldsymbol{x}}^{\mathrm{T}}\tilde{\boldsymbol{P}}\tilde{\boldsymbol{S}}\tilde{\boldsymbol{\varphi}}+\tilde{\boldsymbol{\varphi}}^{\mathrm{T}}\boldsymbol{S}^{\mathrm{T}}\boldsymbol{P}\tilde{\boldsymbol{x}}-\eta^2\tilde{\boldsymbol{\varphi}}^{\mathrm{T}}\tilde{\boldsymbol{\varphi}}\leqslant 0 \tag{18}$$

or equivalently

$$\begin{bmatrix}\tilde{\boldsymbol{x}}\\ \tilde{\boldsymbol{\varphi}}\end{bmatrix}\begin{bmatrix}\tilde{\boldsymbol{A}}^{\mathrm{T}}\tilde{\boldsymbol{P}}+\tilde{\boldsymbol{P}}\tilde{\boldsymbol{A}}+\tilde{\boldsymbol{Q}} & \tilde{\boldsymbol{P}}\tilde{\boldsymbol{S}}\\ \boldsymbol{S}^{\mathrm{T}}\boldsymbol{P} & -\eta^2\boldsymbol{I}\end{bmatrix}\begin{bmatrix}\tilde{\boldsymbol{x}}\\ \tilde{\boldsymbol{\varphi}}\end{bmatrix}\leqslant 0 \tag{19}$$

The goal is now to obtain a tractable LMI problem that allows searching the gain matrices (both the control matrix $\boldsymbol{K}$ and the observer gain matrix $\boldsymbol{L}$) to prove the closed-loop stability (finding $\tilde{\boldsymbol{P}}>0$ to ensure the prescribed attenuation level η).

Remark Most of former results just consider the wireless communication or GPS fault of the multiple aircrafts formation[14,17], but few attempts have been made towards solving the controller design problem with sensor faults. Thus, the novelty of model (Eq. (13)) with respect to existing results is that the sensor fault of FFCS is taken into consideration.

2 Fault Tolerant Control Design

In this section, the fault tolerant formation controller design problem of multiple UAVs is investigated. The design requirements mentioned above are analyzed separately, and the obtained results are utilized for the tracking controller design.

Lemma 1[25] For real matrices $\boldsymbol{X}$, $\boldsymbol{Y}$ and $\boldsymbol{S}=\boldsymbol{S}^{\mathrm{T}}>0$ with appropriate dimensions and a positive constant γ, the following inequalities hold

$$\boldsymbol{X}^{\mathrm{T}}\boldsymbol{Y}+\boldsymbol{Y}^{\mathrm{T}}\boldsymbol{X}\leqslant\gamma\boldsymbol{X}^{\mathrm{T}}\boldsymbol{X}+\gamma^{-1}\boldsymbol{Y}^{\mathrm{T}}\boldsymbol{Y} \tag{20}$$

$$\boldsymbol{X}^{\mathrm{T}}\boldsymbol{Y}+\boldsymbol{Y}^{\mathrm{T}}\boldsymbol{X}\leqslant\boldsymbol{X}^{\mathrm{T}}\boldsymbol{S}^{-1}\boldsymbol{X}+\boldsymbol{Y}^{\mathrm{T}}\boldsymbol{S}\boldsymbol{Y} \tag{21}$$

Lemma 2[26] For real matrices $\boldsymbol{A},\boldsymbol{B},\boldsymbol{W},\boldsymbol{Y},\boldsymbol{Z}$ and a regular matrix $\boldsymbol{Q}$ with appropriate dimensions, one has

$$\begin{bmatrix}\boldsymbol{Y}+\boldsymbol{B}^{\mathrm{T}}\boldsymbol{Q}^{-1}\boldsymbol{B} & \boldsymbol{W}^{\mathrm{T}}\\ \boldsymbol{W} & \boldsymbol{Z}+\boldsymbol{AQA}^{\mathrm{T}}\end{bmatrix}<0\Rightarrow \begin{bmatrix}\boldsymbol{Y} & \boldsymbol{W}^{\mathrm{T}}+\boldsymbol{B}^{\mathrm{T}}\boldsymbol{A}^{\mathrm{T}}\\ \boldsymbol{W}+\boldsymbol{AB} & \boldsymbol{Z}\end{bmatrix}<0 \tag{22}$$

Lemma 3[27] Let a matrix $\boldsymbol{\Xi}<0$, a matrix $\boldsymbol{X}$ with appropriate dimension such that $\boldsymbol{X}^{\mathrm{T}}\boldsymbol{\Xi}\boldsymbol{X}\leqslant 0$, and a scalar α, the following inequality holds

$$\boldsymbol{X}^{\mathrm{T}}\boldsymbol{\Xi}\boldsymbol{X}\leqslant-\alpha(\boldsymbol{X}^{\mathrm{T}}+\boldsymbol{X})-\alpha^2\boldsymbol{\Xi}^{-1}$$

Lemmas 1—3 formulate the conditions under which the inequality meets the negative definite. Based on these propositions, the following theorem presents a controller design method via convex optimization.

Theorem 2 When the sensor fault parameter matrix $\boldsymbol{F}$ of closed-loop system (Eq. (13)) is unknown and satisfies Eqs. (3)—(5), if there exist positive symmetric matrices $\boldsymbol{P}_1=\boldsymbol{P}_1^{\mathrm{T}}>0$, $\boldsymbol{P}_3=\boldsymbol{P}_3^{\mathrm{T}}>0$, $\boldsymbol{N}=\boldsymbol{N}^{\mathrm{T}}>0$, $\boldsymbol{S}=\boldsymbol{S}^{\mathrm{T}}>0$, real matrices $\boldsymbol{Y}$ and $\boldsymbol{Z}$, a positive constant η, such that the following LMI conditions are satisfied

$$\begin{bmatrix} \boldsymbol{\Gamma}_{11}^1 & 0 & \boldsymbol{\Gamma}_{13}^1 & \boldsymbol{P}_1\boldsymbol{\Theta} & 0 & \boldsymbol{Z} & 0 & 0 & \boldsymbol{Z} & 0 \\ * & \boldsymbol{\Gamma}_{22}^1 & 0 & 0 & 0 & 0 & \boldsymbol{NQ} & \hat{\boldsymbol{\Gamma}}_{28}^1 & 0 & \boldsymbol{NC}^{\mathrm{T}} \\ * & * & \hat{\boldsymbol{\Gamma}}_{33}^1 & 0 & 0.5\boldsymbol{P}_3 & 0 & 0 & 0 & 0 & 0 \\ * & * & * & -0.5\eta^2\boldsymbol{I} & 0 & 0 & 0 & 0 & 0 & 0 \\ * & * & * & * & -0.5\eta^2\boldsymbol{I} & 0 & 0 & 0 & 0 & 0 \\ * & * & * & * & * & -\boldsymbol{I} & 0 & 0 & 0 & 0 \\ * & * & * & * & * & * & -2\boldsymbol{Q} & 0 & 0 & 0 \\ * & * & * & * & * & * & * & \boldsymbol{S}-\boldsymbol{I} & 0 & 0 \\ * & * & * & * & * & * & * & * & -\boldsymbol{S}\widetilde{\boldsymbol{F}}^{-2} & 0 \\ * & * & * & * & * & * & * & * & * & -\boldsymbol{S}\widetilde{\boldsymbol{F}}^{-2} \end{bmatrix} < 0 \tag{23}$$

where $\boldsymbol{\Gamma}_{11}^1=0.5[\boldsymbol{P}_1\boldsymbol{A}-\boldsymbol{ZC}+(\boldsymbol{P}_1\boldsymbol{A}-\boldsymbol{ZC})^{\mathrm{T}}]$, $\boldsymbol{\Gamma}_{13}^1=\boldsymbol{Z}(\boldsymbol{I}-\boldsymbol{F}_0)\boldsymbol{C}$, $\boldsymbol{\Gamma}_{22}^1=0.5[\boldsymbol{AN}+\boldsymbol{BY}+(\boldsymbol{AN}+\boldsymbol{BY})^{\mathrm{T}}]$, $\hat{\boldsymbol{\Gamma}}_{33}^1=0.5(\boldsymbol{P}_3\boldsymbol{A}_r+\boldsymbol{A}_r^{\mathrm{T}}\boldsymbol{P}_3)+\boldsymbol{C}^{\mathrm{T}}\boldsymbol{SC}$, $\hat{\boldsymbol{\Gamma}}_{28}^1=\boldsymbol{N}^{\mathrm{T}}\boldsymbol{C}^{\mathrm{T}}(\boldsymbol{I}-\boldsymbol{F}_0)^{\mathrm{T}}$.

$$\begin{bmatrix} \boldsymbol{\Gamma}_{11}^2 & \boldsymbol{I} & 0 & 0 & 0 & 0 & 0 & 0 \\ * & -2\boldsymbol{N} & 0 & 0 & 0 & 0 & 0 & \boldsymbol{Y}^{\mathrm{T}} \\ * & * & \boldsymbol{\Gamma}_{33}^2 & \boldsymbol{A}-\boldsymbol{A}_r & \boldsymbol{\Theta} & -\boldsymbol{I} & \boldsymbol{N}^{\mathrm{T}}\boldsymbol{Q} & 0 \\ * & * & * & \boldsymbol{\Gamma}_{44}^2 & 0 & 0.5\boldsymbol{P}_3 & 0 & 0 \\ * & * & * & * & -0.5\eta^2\boldsymbol{I} & 0 & 0 & 0 \\ * & * & * & * & * & -0.5\eta^2\boldsymbol{I} & 0 & 0 \\ * & * & * & * & * & * & -2\boldsymbol{Q} & 0 \\ * & * & * & * & * & * & * & -\boldsymbol{I} \end{bmatrix} < 0 \tag{24}$$

where $\boldsymbol{\Gamma}_{11}^2=0.5[\boldsymbol{P}_1\boldsymbol{A}-\boldsymbol{ZC}+(\boldsymbol{P}_1\boldsymbol{A}-\boldsymbol{ZC})^{\mathrm{T}}]$, $\boldsymbol{\Gamma}_{33}^2=0.5[\boldsymbol{AN}+\boldsymbol{BY}+(\boldsymbol{AN}+\boldsymbol{BY})^{\mathrm{T}}]+\boldsymbol{BB}^{\mathrm{T}}$, $\boldsymbol{\Gamma}_{44}^2=0.5\cdot(\boldsymbol{P}_3\boldsymbol{A}_r+\boldsymbol{A}_r^{\mathrm{T}}\boldsymbol{P}_3)$. Then the asymptotic stability of the closed-loop formation control system (Eq. (13)) is ensured and the H_∞ tracking control performance (Eq. (14)) is guaranteed with an attenuation level η. Moreover, if a solution exists, the gains $\boldsymbol{K}$ and $\boldsymbol{L}$ are obtained using $\boldsymbol{K}=\boldsymbol{YN}^{-1}$ and $\boldsymbol{L}=\boldsymbol{P}^{-1}\boldsymbol{Z}$.

Proof Assuming that $\widetilde{\boldsymbol{P}}=\mathrm{diag}\{\boldsymbol{P}_1,\boldsymbol{P}_2,\boldsymbol{P}_3\}$ and $\boldsymbol{P}_2=\boldsymbol{P}_2^{\mathrm{T}}>0$, in-Eq. (19) can be rewritten as

$$\begin{bmatrix} \boldsymbol{\Pi}_{11} & \boldsymbol{\Pi}_{12} & \boldsymbol{P}_1\boldsymbol{L}(\boldsymbol{I}-\boldsymbol{F})\boldsymbol{C} & \boldsymbol{P}_1\boldsymbol{\Theta} & 0 \\ * & \boldsymbol{\Pi}_{22} & \boldsymbol{P}_2(\boldsymbol{A}-\boldsymbol{A}_r) & \boldsymbol{P}_2\boldsymbol{\Theta} & -\boldsymbol{P}_2 \\ * & * & \boldsymbol{P}_3\boldsymbol{A}_r+\boldsymbol{A}_r^{\mathrm{T}}\boldsymbol{P}_3 & 0 & \boldsymbol{P}_3 \\ * & * & * & -\eta^2\boldsymbol{I} & 0 \\ * & * & * & * & -\eta^2\boldsymbol{I} \end{bmatrix} < 0 \tag{25}$$

where

$\boldsymbol{\Pi}_{11}=\boldsymbol{P}_1(\boldsymbol{A}-\boldsymbol{LC})+(\boldsymbol{A}-\boldsymbol{LC})^{\mathrm{T}}\boldsymbol{P}_1$, $\boldsymbol{\Pi}_{12}=\boldsymbol{P}_1\boldsymbol{L}(\boldsymbol{I}-\boldsymbol{F})\boldsymbol{C}+\boldsymbol{K}^{\mathrm{T}}\boldsymbol{B}^{\mathrm{T}}\boldsymbol{P}_2$, $\boldsymbol{\Pi}_{22}=\boldsymbol{P}_2(\boldsymbol{A}+\boldsymbol{BK})+(\boldsymbol{A}+\boldsymbol{BK})^{\mathrm{T}}\boldsymbol{P}_2+\boldsymbol{Q}$

For a convenient design, in-Eq. (19) is simplified as

$$\boldsymbol{\Gamma}^1+\boldsymbol{\Gamma}^2<0$$

where

$$\boldsymbol{\Gamma}^1=\begin{bmatrix} \bar{\boldsymbol{\Gamma}}_{11}^1 & \boldsymbol{P}_1\boldsymbol{L}(\boldsymbol{I}-\boldsymbol{F})\boldsymbol{C} & \boldsymbol{P}_1\boldsymbol{L}(\boldsymbol{I}-\boldsymbol{F})\boldsymbol{C} & \boldsymbol{P}_1\boldsymbol{\Theta} & 0 \\ * & \bar{\boldsymbol{\Gamma}}_{22}^1 & 0 & 0 & 0 \\ * & * & 0.5(\boldsymbol{P}_3\boldsymbol{A}_r+\boldsymbol{A}_r^{\mathrm{T}}\boldsymbol{P}_3) & 0 & 0.5\boldsymbol{P}_3 \\ * & * & * & -0.5\eta^2\boldsymbol{I} & 0 \\ * & * & * & * & -0.5\eta^2\boldsymbol{I} \end{bmatrix}$$

$$\boldsymbol{\Gamma}^2=\begin{bmatrix} \bar{\boldsymbol{\Gamma}}_{11}^2 & \boldsymbol{K}^{\mathrm{T}}\boldsymbol{B}^{\mathrm{T}}\boldsymbol{P}_2 & 0 & 0 & 0 \\ * & \bar{\boldsymbol{\Gamma}}_{22}^2 & \boldsymbol{P}_2(\boldsymbol{A}-\boldsymbol{A}_r) & \boldsymbol{P}_2\boldsymbol{\Theta} & -\boldsymbol{P}_2 \\ * & * & 0.5(\boldsymbol{P}_3\boldsymbol{A}_r+\boldsymbol{A}_r^{\mathrm{T}}\boldsymbol{P}_3) & 0 & 0.5\boldsymbol{P}_3 \\ * & * & * & -0.5\eta^2\boldsymbol{I} & 0 \\ * & * & * & * & -0.5\eta^2\boldsymbol{I} \end{bmatrix}$$

$\bar{\boldsymbol{\Gamma}}_{11}^1=0.5[\boldsymbol{P}_1(\boldsymbol{A}-\boldsymbol{LC})+(\boldsymbol{A}-\boldsymbol{LC})^{\mathrm{T}}\boldsymbol{P}_1]$, $\bar{\boldsymbol{\Gamma}}_{22}^1=0.5\cdot[\boldsymbol{P}_2(\boldsymbol{A}+\boldsymbol{BK})+(\boldsymbol{A}+\boldsymbol{BK})^{\mathrm{T}}\boldsymbol{P}_2+\boldsymbol{Q}]$, $\bar{\boldsymbol{\Gamma}}_{11}^2=0.5[\boldsymbol{P}_1(\boldsymbol{A}-\boldsymbol{LC})+(\boldsymbol{A}-\boldsymbol{LC})^{\mathrm{T}}\boldsymbol{P}_1]$, $\bar{\boldsymbol{\Gamma}}_{22}^2=0.5[\boldsymbol{P}_2(\boldsymbol{A}+\boldsymbol{BK})+(\boldsymbol{A}+\boldsymbol{BK})^{\mathrm{T}}\boldsymbol{P}_2+\boldsymbol{Q}]$.

Then in-Eq. (25) holds, if $\boldsymbol{\Gamma}^1<0$ and $\boldsymbol{\Gamma}^2<0$.

Using the well-known property in Lemma 1, the following inequality can be deduced

$$\boldsymbol{e}_0^{\mathrm{T}}\boldsymbol{P}_1\boldsymbol{L}(\boldsymbol{I}-\boldsymbol{F})\boldsymbol{C}\boldsymbol{e}_p+\boldsymbol{e}_p^{\mathrm{T}}\boldsymbol{C}^{\mathrm{T}}(\boldsymbol{I}-\boldsymbol{F})\boldsymbol{L}^{\mathrm{T}}\boldsymbol{P}_1\boldsymbol{e}_0\leqslant \boldsymbol{e}_0^{\mathrm{T}}\boldsymbol{P}_1\boldsymbol{L}(\boldsymbol{P}_1\boldsymbol{L})^{\mathrm{T}}\boldsymbol{e}_0+\boldsymbol{e}_p^{\mathrm{T}}\boldsymbol{C}^{\mathrm{T}}(\boldsymbol{I}-\boldsymbol{F})^{\mathrm{T}}(\boldsymbol{I}-\boldsymbol{F})\boldsymbol{C}\boldsymbol{e}_p$$

Based on the above, $\boldsymbol{\Gamma}^1<0$ is equivalent to

$$\widetilde{\boldsymbol{\Gamma}}^1=\begin{bmatrix}\widetilde{\boldsymbol{\Gamma}}_{11}^1 & 0 & \boldsymbol{P}_1\boldsymbol{L}(\boldsymbol{I}-\boldsymbol{F})\boldsymbol{C} & \boldsymbol{P}_1\boldsymbol{\Theta} & 0\\ * & \widetilde{\boldsymbol{\Gamma}}_{22}^1 & 0 & 0 & 0\\ * & * & 0.5(\boldsymbol{P}_3\boldsymbol{A}_r+\boldsymbol{A}_r^{\mathrm{T}}\boldsymbol{P}_3) & 0 & 0.5\boldsymbol{P}_3\\ * & * & * & -0.5\eta^2\boldsymbol{I} & 0\\ * & * & * & * & -0.5\eta^2\boldsymbol{I}\end{bmatrix}<0 \tag{26}$$

where $\widetilde{\boldsymbol{\Gamma}}_{22}^1=0.5[\boldsymbol{P}_2(\boldsymbol{A}+\boldsymbol{BK})+(\boldsymbol{A}+\boldsymbol{BK})^{\mathrm{T}}\boldsymbol{P}_2+\boldsymbol{Q}]+\boldsymbol{C}^{\mathrm{T}}(\boldsymbol{I}-\boldsymbol{F})^{\mathrm{T}}(\boldsymbol{I}-\boldsymbol{F})\boldsymbol{C}$, $\widetilde{\boldsymbol{\Gamma}}_{11}^1=0.5[\boldsymbol{P}_1(\boldsymbol{A}-\boldsymbol{LC})+(\boldsymbol{A}-\boldsymbol{LC})^{\mathrm{T}}\boldsymbol{P}_1]+\boldsymbol{P}_1\boldsymbol{L}(\boldsymbol{P}_1\boldsymbol{L})^{\mathrm{T}}$.

Then, one proceeds a bijective change of variables followed by a pre-post multiply of the in-Eq. (26) by diag$\{\boldsymbol{I},\boldsymbol{N},\boldsymbol{I},\boldsymbol{I},\boldsymbol{I}\}$ with $\boldsymbol{Z}=\boldsymbol{P}_1\boldsymbol{L},\boldsymbol{N}=\boldsymbol{P}_2^{-1}$ and $\boldsymbol{KP}_2^{-1}=\boldsymbol{KN}=\boldsymbol{Y}$, and obtains

$$\begin{bmatrix}\boldsymbol{\Gamma}_{11}^1 & 0 & \boldsymbol{Z}(\boldsymbol{I}-\boldsymbol{F})\boldsymbol{C} & \boldsymbol{P}_1\boldsymbol{\Theta} & 0 & \boldsymbol{Z} & 0 & 0\\ * & \boldsymbol{\Gamma}_{22}^1 & 0 & 0 & 0 & 0 & \boldsymbol{N}^{\mathrm{T}}\boldsymbol{Q} & \boldsymbol{\Gamma}_{28}^1\\ * & * & \boldsymbol{\Gamma}_{33}^1 & 0 & 0.5\boldsymbol{P}_3 & 0 & 0 & 0\\ * & * & * & -0.5\eta^2\boldsymbol{I} & 0 & 0 & 0 & 0\\ * & * & * & * & -0.5\eta^2\boldsymbol{I} & 0 & 0 & 0\\ * & * & * & * & * & -\boldsymbol{I} & 0 & 0\\ * & * & * & * & * & * & -2\boldsymbol{Q} & 0\\ * & * & * & * & * & * & * & -\boldsymbol{I}\end{bmatrix}<0 \tag{27}$$

where $\boldsymbol{\Gamma}_{11}^1=0.5[\boldsymbol{P}_1\boldsymbol{A}-\boldsymbol{ZC}+(\boldsymbol{P}_1\boldsymbol{A}-\boldsymbol{ZC})^{\mathrm{T}}]$, $\boldsymbol{\Gamma}_{22}^1=0.5[\boldsymbol{AN}+\boldsymbol{BY}+(\boldsymbol{AN}+\boldsymbol{BY})^{\mathrm{T}}]$, $\boldsymbol{\Gamma}_{33}^1=0.5(\boldsymbol{P}_3\boldsymbol{A}_r+\boldsymbol{A}_r^{\mathrm{T}}\boldsymbol{P}_3)$, $\boldsymbol{\Gamma}_{28}^1=\boldsymbol{N}^{\mathrm{T}}\boldsymbol{C}^{\mathrm{T}}(\boldsymbol{I}-\boldsymbol{F})^{\mathrm{T}}$.

Similarly, $\boldsymbol{\Gamma}^2<0$ can be turned into

$$\boldsymbol{\Gamma}^2=\begin{bmatrix}\boldsymbol{\Gamma}_{11}^2 & \boldsymbol{I} & 0 & 0 & 0 & 0 & 0 & 0\\ * & -2\boldsymbol{N} & 0 & 0 & 0 & 0 & 0 & \boldsymbol{Y}^{\mathrm{T}}\\ * & * & \boldsymbol{\Gamma}_{33}^2 & \boldsymbol{A}-\boldsymbol{A}_r & \boldsymbol{\Theta} & -\boldsymbol{I} & \boldsymbol{N}^{\mathrm{T}}\boldsymbol{Q} & 0\\ * & * & * & 0.5(\boldsymbol{P}_3\boldsymbol{A}_r+\boldsymbol{A}_r^{\mathrm{T}}\boldsymbol{P}_3) & 0 & 0.5\boldsymbol{P}_3 & 0 & 0\\ * & * & * & * & -0.5\eta^2\boldsymbol{I} & 0 & 0 & 0\\ * & * & * & * & * & -0.5\eta^2\boldsymbol{I} & 0 & 0\\ * & * & * & * & * & * & -2\boldsymbol{Q} & 0\\ * & * & * & * & * & * & * & -\boldsymbol{I}\end{bmatrix}<0 \tag{28}$$

where $\boldsymbol{\Gamma}_{11}^2=0.5(\boldsymbol{P}_1\boldsymbol{A}-\boldsymbol{ZC})+0.5(\boldsymbol{P}_1\boldsymbol{A}-\boldsymbol{ZC})^{\mathrm{T}}$, $\boldsymbol{\Gamma}_{33}^2=0.5[\boldsymbol{AN}+\boldsymbol{BY}+(\boldsymbol{AN}+\boldsymbol{BY})^{\mathrm{T}}]+\boldsymbol{BB}^{\mathrm{T}}$.

Using Eqs. (3)—(5), in-Eq. (27) can be rewritten as

$$\boldsymbol{M}^1=\boldsymbol{M}_0^1+\boldsymbol{\xi}\boldsymbol{F}_\delta\boldsymbol{\beta}^{\mathrm{T}}+\boldsymbol{\beta}\boldsymbol{F}_\delta\boldsymbol{\xi}^{\mathrm{T}}+\boldsymbol{\mu}\boldsymbol{F}_\delta\boldsymbol{\upsilon}^{\mathrm{T}}+\boldsymbol{\upsilon}\boldsymbol{F}_\delta\boldsymbol{\mu}^{\mathrm{T}}<0 \tag{29}$$

$$\boldsymbol{M}_0^1=\begin{bmatrix}\boldsymbol{\Gamma}_{11}^1 & 0 & \boldsymbol{Z}(\boldsymbol{I}-\boldsymbol{F}_0)\boldsymbol{C} & \boldsymbol{P}_1\boldsymbol{\Theta} & 0 & \boldsymbol{Z} & 0 & 0\\ * & \boldsymbol{\Gamma}_{22}^1 & 0 & 0 & 0 & 0 & \boldsymbol{N}^{\mathrm{T}}\boldsymbol{Q} & \hat{\boldsymbol{\Gamma}}_{28}^1\\ * & * & \boldsymbol{\Gamma}_{33}^1 & 0 & 0.5\boldsymbol{P}_3 & 0 & 0 & 0\\ * & * & * & -0.5\eta^2\boldsymbol{I} & 0 & 0 & 0 & 0\\ * & * & * & * & -0.5\eta^2\boldsymbol{I} & 0 & 0 & 0\\ * & * & * & * & * & -\boldsymbol{I} & 0 & 0\\ * & * & * & * & * & * & -2\boldsymbol{Q} & 0\\ * & * & * & * & * & * & * & -\boldsymbol{I}\end{bmatrix}$$

where $\boldsymbol{\xi}=[-\boldsymbol{Z}^{\mathrm{T}},0,0,0,0,0,0,0]^{\mathrm{T}}$, $\boldsymbol{\beta}=[0,0,\boldsymbol{C},0,0,0,0,0]^{\mathrm{T}}$, $\hat{\boldsymbol{\Gamma}}_{28}^1=\boldsymbol{N}^{\mathrm{T}}\boldsymbol{C}^{\mathrm{T}}(\boldsymbol{I}-\boldsymbol{F}_0)^{\mathrm{T}}$, $\boldsymbol{\upsilon}=[0,0,0,0,0,0,0,\boldsymbol{I}]^{\mathrm{T}}$ and $\boldsymbol{\mu}=[0,-\boldsymbol{CN},0,0,0,0,0,0,0]^{\mathrm{T}}$.

For Lemma 1 and $\boldsymbol{S}=\boldsymbol{S}^{\mathrm{T}}>0$, in-Eq. (29) is equivalent to

$$\boldsymbol{M}^1\leqslant\boldsymbol{M}_0^1+\boldsymbol{\xi}\boldsymbol{S}^{-1}\widetilde{\boldsymbol{F}}^2\boldsymbol{\xi}^{\mathrm{T}}+\boldsymbol{\beta}\boldsymbol{S}\boldsymbol{\beta}^{\mathrm{T}}+\boldsymbol{\mu}\boldsymbol{S}^{-1}\widetilde{\boldsymbol{F}}^2\boldsymbol{\mu}^{\mathrm{T}}+\boldsymbol{\upsilon}\boldsymbol{S}\boldsymbol{\upsilon}^{\mathrm{T}}$$

Applying Schur complement theorem on the above inequalities, the in-Eq. (23) is deduced, then Theorem 3 is proved. When sensor fault of FFCS is unknown and satisfies conditions (Eqs. (3)—(5)), the asymptotic stability of the close-loop FFCS (Eq. (13)) is ensured.

3 Simulation Results

Simulations are performed for FFCS consisting of two UAVs. The expected formation geometries are specified by $x_c=20$ m, $y_c=20$ m and $z_c=0$ m, respectively. The initial state of leader UAV are set as: $V_{L_0}=30$ m/s, $\psi_{L_0}=10°$, $h_{L_0}=1\ 000$ m. The initial state of follower UAV are set as: $V_{W_0}=20$ m/s, $\psi_{W_0}=20°$, $h_{W_0}=1\ 010$ m. The initial formation geometries are defined as: $x_0=35$ m, $y_0=35$ m and $z_0=-10$ m. The dynamic matrices $\boldsymbol{A}$ and $\boldsymbol{B}$ are valuated for the data listed as[8]: The velocity time constant $\tau_{V_W}=5$ s, the heading time constant $\tau_{\psi_W}=0.75$ s, the altitude time constant $\tau_{h_a}=0.3$ s, $\tau_{h_b}=3.85$ s. Outside disturbance is assumed as: $\boldsymbol{w}_2=0.02\cdot[2\sin t, \cos 0.5t, 3\sin t-\cos t]^{\mathrm{T}}$. Furthermore, the parameter matrix of the reference model is given by

$$\boldsymbol{A}_r=\begin{bmatrix} 0.563\,7 & -1.068\,3 & 2.877\,4 & -9.422 & 0 & 0 \\ -8.450\,3 & 0.202\,7 & 0 & 0 & 0.629\,6 & 0 \\ 0 & 0 & -2.953\,4 & -6.812\,9 & 0 & 0 \\ 0 & 0 & -0.691\,2 & -3.177\,5 & 0 & 0 \\ 0 & -1.328\,4 & 0 & 0 & 4.153\,2 & 1.007\,8 \\ -0.735\,9 & 0 & 0 & 0 & 0.630\,4 & -6.182\,4 \end{bmatrix}$$

The resulting design is simulated in Matlab's Simulink package by the mathworks. To verify the superiority of the control approach, it is assumed that unknown sensor faults occur in the sensor channels of x, V_W and y, respectively. It is assumed that $\underline{\boldsymbol{F}}=0.1\ \mathrm{diag}\{1,1,1\}$, $\bar{\boldsymbol{F}}=0.9\cdot\mathrm{diag}\{1,1,1\}$.

In the following, different simulation results are given using a robust controller without FTC and an observer-based FTC scheme developed in this study, respectively. First of all, a robust tracking controller without FTC is adopted. As shown in Figs. 2,3, the robust controller without FTC cannot guarantee the state and control input of FFCS having a satisfactory dynamic performance. For example, the evolution of x cannot asymptotically track command x_c.

Correspondingly, according to the linear matrix inequality in Theorem 3, one can deduce the fault tolerant tracking controller matrix $\boldsymbol{K}$ and observer gain matrix $\boldsymbol{L}$ as

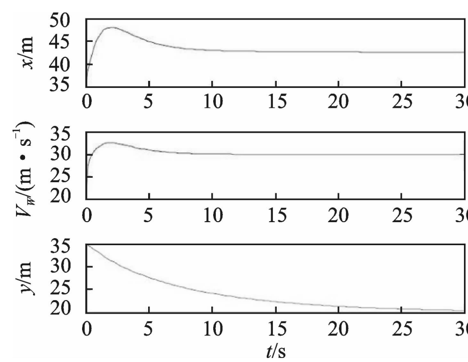

Fig. 2 State evolution of FFCS using controller without FTC

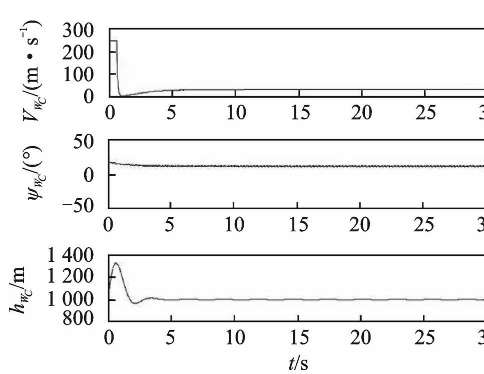

Fig. 3 Control input evolution of FFCS using controller without FTC

$$\boldsymbol{K}=\begin{bmatrix} 0.357\,8 & -7.143\,6 & -2.247\,3 & 7.138\,7 & 13.648\,1 & 14.378\,7 \\ 0.048\,7 & -0.005\,7 & 2.245\,9 & -9.771\,4 & -0.000\,1 & -0.000\,1 \\ -0.088\,9 & 0.410\,4 & -0.003 & 0.180\,4 & -13.688\,4 & -14.483\,6 \end{bmatrix}$$

$$
\boldsymbol{L} = 10^3 \cdot \begin{bmatrix} 5.540\,5 & 6.179\,6 & -9.290\,5 \\ 5.518\,2 & 6.212\,0 & -9.300\,2 \\ 5.407\,1 & 6.058\,7 & -9.040\,7 \\ 5.795\,7 & 6.500\,2 & -9.871\,1 \\ 5.622\,3 & 6.302\,8 & -9.495\,9 \\ 5.618\,7 & 6.298\,9 & -9.492\,5 \end{bmatrix}
$$

By utilizing the robust fault tolerant controller obtained in Theorem 3, it can be seen from Fig. 4 that the unknown sensor fault can be well regulated. Both x and y asymptotically track the specified commands x_c and y_c within 6 s. Moreover, as shown in Fig. 5, the robust fault tolerant tracking controller developed in this paper, makes that control input responses of the close-loop FFCS have a satisfactory dynamic performance in spite of the sensor fault, which demonstrates the efficiency of the proposed approach.

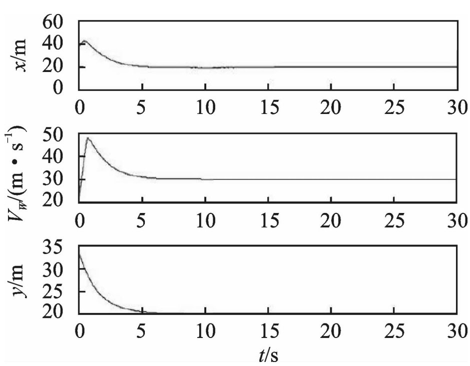

Fig. 4 State evolution of FFCS using robust fault tolerant controller

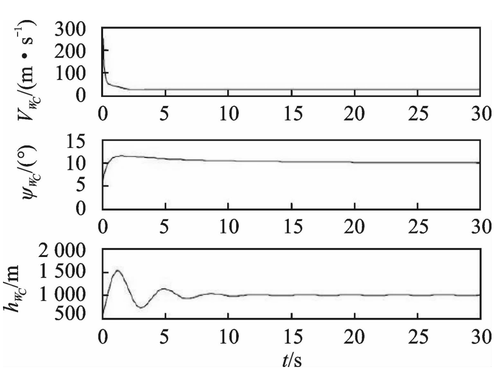

Fig. 5 Control input evolution of FFCS using robust fault tolerant controller

4 Conclusions

In this study, a novel fault tolerant tracking control design approach is proposed for a class of multiple UAVs formation control systems with sensor faults using both LMI technique and Lyapunov stability approach, which guarantees that the faulty UAVs formation has the good fault tolerant capability. Firstly, a formation control model of multiple UAVs considering the disturbances and sensor faults is introduced and a sensor gain fault model is also given. Then a robust fault tolerant tracking controller is designed in unknown sensor faulty case by means of a generalized observer. Finally, the simulation results are shown to exhibit the effectiveness of designed FTC approach.

Acknowledgements

This work was supported in part by the Post Doctoral Research Foundation of Jiangsu Province (No. 1701140B), the National Natural Science Foundation of China (No. 61403195), and the GF Research and Development Project of the Nanjing Tech Universities (No. 201709).

References:

[1] TUNA G, NEFZI B, CONTE G. Unmanned aerial vehicle-aided communications system for disaster recovery [J]. Journal of Network and Computer Applications, 2014, 41(5):27-36.

[2] LI P, YU X, ZHANG Y M, et al. Adaptive multivariable integral TSMC of a hypersonic gliding vehicle with actuator faults and model uncertainties [J]. IEEE/ASME Transactions on Mechatronics, 2017, 22(6):2723-2735.

[3] BAYEZIT I, FIDAN B. Distributed cohesive motion control of flight vehicle formations [J]. IEEE Transactions on Industrial Electronics, 2013, 60(12): 5763-5772.

[4] SHI X Y, QI R Y. Modeling and attitude control for three-axis liquid-filled spacecraft [J]. Journal of Nanjing University of Aeronautics and Astronautics, 2017, 49(1):132-139. (in Chinese)

[5] OH K K, PARK M C, AHN H S. A survey of multi-agent formation control [J]. Automatica, 2015, 53(3):424-440.

[6] DONG L F, CHEN Y Z, QU X J. Formation control strategy for nonholonomic intelligent vehicles based on virtual structure and consensus approach[J]. Procedia Engineering, 2016, 137(4):415-424.

[7] LIU L, SHAN J J. Distributed formation control of networked Euler-lagrange systems with fault diagnosis [J]. Journal of the Franklin Institute, 2015, 352(3):952-973.

[8] MYSTKOWSKI A. Implementation and investiga-

tion of a robust control algorithm for an unmanned microaerial vehicle [J]. Robotics and Autonomous Systems, 2014, 62(8):1187-1196.

[9] XIE C H, YANG G H. Cooperative guaranteed cost fault-tolerant control for multi-agent systems with time-varying actuator faults [J]. Neurocomputing, 2016, 214(11):382-390.

[10] MA C, ZENG Q. Distributed formation control of 6-DOF autonomous underwater vehicles networked by sampled-data information under directed topology [J]. Neurocomputing, 2015, 154(4):33-40.

[11] HE L L, BAI P, LIANG X L, et al. Feedback formation control of UAV swarm with multiple implicit leaders [J]. Aerospace Science and Technology, 2018, 72(1):327-334.

[12] PROUD A, PACHTER W M, AZZO J D. Close formation flight control[C]//Guidance, Navigation, and Control Conference and Exhibit. Portland, OR, USA: [s. n.], 1999:1231-1246.

[13] YU M, WANG H F, XIE G M, et al. Event-triggered circle formation control for second-order-agent system[J]. Neurocomputing, 2018, 275(1):462-469.

[14] INNOCENTI M, POLLINI L, GIULIETTI F. Management of communication failures in formation flight[J]. Journal of Aerospace Computing, Information, and Communication, 2004, 1(1):19-35.

[15] DONG H Y, HU Q L, MA G F. Dual-quaternion based fault-tolerant control for spacecraft formation flying with finite-time convergence[J]. ISA Transactions, 2016, 61(3):87-94.

[16] HUA Y Z, DONG X W, LI Q D, et al. Distributed fault-tolerant time-varying formation control for high-order linear multi-agent systems with actuator failures[J]. ISA Transactions, 2017, 71(12):40-50.

[17] QU Y H, ZHANG Y M. Cooperative localization against GPS signal loss in multiple UAVs flight[J]. Journal of Systems Engineering and Electronics, 2011, 22(1):103-112.

[18] BUONOCORE L R, LIPPIELLO V, MANFREDI S, et al. Effects of packet losses on formation control of unmanned aerial vehicles[C]//Proceedings of the 19th World Congress The International Federation of Automatic Control. Cape Town, South Africa: [s. n.],2014.

[19] YU X, FU Y, PENG X. Fuzzy logic aided fault-tolerant control applied to transport aircraft subject to actuator stuck failures [J]. IEEE Transactions on Fuzzy System, 2017, 25(10):1-11.

[20] YANG A, NAEEM W, IRWIN G W, et al. Stability analysis and implementation of a decentralized formation control strategy for unmanned vehicles [J]. IEEE Transactions on Control Systems Technology, 2014, 22(2):706-720.

[21] YIN S, XIAO B, DING S X, ZHOU D H. A review on recent development of spacecraft attitude fault tolerant control system[J]. IEEE Transactions on Industrial Electronics, 2016, 63(5):3311-3320.

[22] KIM S H, NEGASH L, CHOI H L. Cubature Kalman filter based fault detection and isolation for formation control of multi-UAVs[J]. IFAC Papersonline, 2016, 49(15):63-68.

[23] ZHANG C X, WANG J H, ZHANG D X, et al. Fault tolerant adaptive finite time attitude synchronization and tracking control for multi-spacecraft formation [J]. Aerospace Science and Technology, 2018, 73(2):197-209.

[24] AMBROZIAK L, GOSIEWSKI Z. Two stage switching control for autonomous formation flight of unmanned aerial vehicles[J]. Aerospace Science Technology, 2015, 46(10/11):221-226.

[25] WANG X, YANG G H. Distributed fault tolerant control for a class of cooperative uncertain systems with actuator failures and switching topologies [J]. Information Sciences, 2016, 370/371:650-666.

[26] BUSTON D, PARIZ N, HOSSEINI S S. Robust fault-tolerant tracking control design for spacecraft under control input saturation[J]. ISA Transactions, 2014, 53 (4):1073-1080.

[27] XU J. Fault tolerant finite-time leader-follower formation control for autonomous surface vessels with LOS range and angle constraints [J]. Automatica, 2016, 68(6):228-236.

Dr. **Qian Moshu** is currently an associate professor in Nanjing Tech University. She received the Ph. D. degree in Control Theory and Control Engineering from Nanjing University of Aeronautics and Astronautics. Her research has focused on stability analysis and fault tolerant controller design of the linear or nonlinear system.

Prof. **Xiong Ke** is currently a professor in State Key Laboratory of Mechanics and Control of Mechanical Structures, Nanjing University of Aeronautics and Astronautics. His research has focused on intelligent structure system of aerocraft.

(Production Editor: Sun Jing)